Supporting Information on:

Aggregation-Induced Conformational Transitions in Bovine β-Lactoglobulin Adsorbed on Open Chitosan Structures

João Borges[1], *José M. Campiña* [*1], *Hiléia K. S. Souza* [2], *Maria P. Gonçalves* [2], *A. Fernando Silva* [1]

[1] Centro de Investigação em Química (CIQ). Departamento de Química. Faculdade de Ciências. Universidade do Porto. Rua do Campo Alegre 687, 4169-007 Porto, Portugal

[2] REQUIMTE. Departamento Engenharia Química. Faculdade de Engenharia. Universidade do Porto. Rua Dr. Roberto Frias, 4200-465, Porto, Portugal

[*] *Corresponding author:* José Miguel Campiña, Email: jpina@fc.up.pt

S1 The Sauerbrey´s equation

According to Sauerbrey et al.,[1] the shift in the vibration frequency (Δf) suffered by a quartz plate in air is associated to both changes in the crystal and in the deposited mass (Δm) on it:

$$\Delta f / n = [-2 f_0^2 / A (p_q m_q)^{1/2}] \Delta m = - (C_f / A) \Delta m \quad (1)$$

where f_0 is the resonant frequency of the quartz plate (here 5 MHz), A the piezoelectrically active area (defined by the gold covered surface, A = 0.785 cm^2), $p_q m_q$ the product of the density (2.648 g cm^{-3}) and the shear modulus of quartz (2.947×10^{11} g cm^{-1} s^{-2}) respectively, and n the overtone number. C_f is called the sensitivity factor of the crystals and has a value of 55.5 Hz mg^{-1} cm^2 at room temperature for the quartz plates previously described.

Equation 1 supposes that the deposited mass must be rigid (with no energy dissipation) and evenly distributed. Thin films meeting these requirements ensure that viscoelastic effects and/or overadsorption do not affect significantly the results, thus, enabling the application of equation 1 for the quantitative analysis of the adsorption phenomena.

We found in our previous research that for high values of I and β-LG concentration, pH changes can promote the formation of large aggregates (overadsorption), turning the films highly viscoelastic and unable to follow the oscillation rigidly.[2] This behavior agrees well with that observed in the adsorption of other proteins on solid surfaces.[3-5] Under these conditions the dissipation energy can change significantly and that must be taken into consideration to make a complete interpretation of the adsorption phenomena. As better discussed in the manuscript, there other factors that affect the viscoelasticity of the layers. Especifically, when working with proteins trapped water is an important factor leading to the overstimation of the mass measured by QCM.

S2. Preparation and characterization of chitosan surfaces

S2.1 Preparation of chitosan-decorated Au surfaces

Prior to each experiment the gold-covered quartz plates were cleaned at room temperature (20º C) with freshly prepared piranha solution (3:1 = H_2SO_4/30% H_2O_2, v/v) for 2 min to remove impurities, later rinsed with large amounts of ethanol and Millipore water, and then dryed under a stream of nitrogen. *Piranha solution is very corrosive, reacts violently with organic materials and utmost care should be taken and proper protective clothing should be used when handling it. Piranha solution should be handled with extreme care, and only small volumes should be prepared at any time.* In all cases, the quartz crystals were used immediately after the cleaning process.

The methodology used to prepare chitosan-modified surfaces consists in the well-known Layer by Layer (LbL) deposition of oppositely charged polyelectrolytes (Scheme 1). The QCM-D crystals were inserted into the cell exposing just one side of the quartz plate for measurements. After probe equilibration in air, and then in ethanol, a 1 mM AUT solution was injected into the QCM-D cell and the variations in f and D were registered until stabilization. Proper equilibration was indicated by cessation of any significant further decrease in the frequency of the plates. Afterwards, pure acetate buffer 0.05 M (pH=5.5) was injected until equilibration. Then the deposition of each polyelectrolyte was performed starting by pSS. At this point, a 1 mg·mL^{-1} solution of pSS in the same buffer was injected and measurements taken until equilibration. In an analogous way, pure buffer and 1 mg·mL^{-1} Chit95 solution were succesively injected into the cell. After each deposition step, and before equilibration in the liquid phase (buffer), the plates were removed from the cell, rinsed with ultrapure water (in order to remove the unbounded polymer and traces of acetic acid), and dried under N_2 for further ex-situ characterization. Good stability and reproducibility have been demonstrated for chitosan films prepared in this way.[2] In the last step, β-LG solutions with different protein concentration in the same buffer were injected to follow the adsorption process. The whole process was repeated at each protein concentration.

S2.2 Energy dissipation data

The shift in the dissipation factor (DD_n) was measured, in simultanous with the

shifts in resonance frequency (Df_n), during the LbL deposition of the different layers composing the Au/AUT/pSS/chit95 surfaces by means of the QCM-D technique (Figures S1 and S2).

S2.3 Atomic Force Microscopy

Topographic 5 x 5 μm^2 AFM pictures recorded in tapping mode at the different stages of the modification of the plates with the pSS-chit95 bilayer are presented in Figure S3. The statistical information on the roughness, height, and particle size derived from them are shown in Table S1.

S2.4 Scanning Electron Microscopy (SEM)

SEM pictures were taken over regions of different dimensions for both, Au/AUT/pSS and Au/AUT/pSS/chit95 surfaces, in a high-vacuum (20 kV) and through the analysis of secondary electrons (SE mode) using a FEI Quanta 400 FEG microscope (Figure S4). The very same QCM-D quartz plates previously modified with the multilayer assembly and exposed to the different protein solutions, were rinsed in ultrapure water, dried under a stream of N_2, and mounted on aluminum stubs covered with double-coated carbon conductive adhesive tabs for electrical contact purposes.

S2.5 Contact Angle Pictures

The wettability of Au substrates functionalized with AUT, AUT/pSS, and AUT/pSS/Chit95 was determined through the static sessile drop method using a contact-angle goniometer formed by an Olympus SZH8 zoom microscope coupled to a Panasonic WV-BL200 camera and the software Optimas 4.01. Ultrapure water was used as the liquid phase and polycrystalline Au slides as the modified substrates. The different images taken are presented in Figure S5. The freeware ImageJ was used for the analysis of surface-drop contact angles at each surface. The results for three drops (5 μL) were averaged for each surface as shown in Table 1 in the manuscript.

S3. Random Sequential Adsorption Theory

Adsorption of β-LG onto Au/AUT and Au/AUT/pSS/chit95 surfaces was analyzed using a simplified form of the RSA model. But let us first to evaluate the viability of

using a much simpler formalism such as the Langmuir kinetic model. According to the latter, the adsorption rate, $d\theta/dt$, is reduced with decreasing the amount of available binding sites (1-θ) on the surface. Supposing irreversible adsorption this kinetic law can be expressed as:

$$d\theta/dt = k_{ON} C_b (1-\theta) \qquad (2)$$

It is implicitly assumed that the surface is composed of a finite number of adsorption sites and that each molecule can interact only with one of these sites (site-specific adsorption), otherwise the available area for the adsorption of a new particle cannot be longer given by $(1-\theta)$. Large molecules such as proteins occupy a large number of sites (non-site-specific) and the surface needs to be treated as a continuum ("planar" or "molecularly flat" surface). This is usually done using an empirical generalized Langmuir equation:

$$d\theta/dt = k_{ON} C_b (1-\theta/\theta_M) \qquad (3)$$

However, there is a general accordance in the field that this formalism is not adequate to describe protein adsorption phenomena. The Langmuir model can not account for certain kind of phenomena related with the non-site-specific nature of the adsorption process, such as surface exclusion effects induced by pre-adsorbed proteins (often referred to as negative cooperativity).

Substituting the term (1-θ/θ_M) by a function $\Phi(\theta)$, so-called the available surface function, which provides with a more realistic depletion of surface sites and consider the adsorption of protein to random surface sites may overtake some of the limitations of the Langmuir model. Up to date an exact solution for this function has been just obtained for the one dimensional (1D) adsorption or the so-called *Random Parking* problem.[6] Talbot and Schaaf derived an approximate solution for the 2D problem considering hard discs to model the particles:[7]

$$\Phi(\theta) = (1-\theta/\theta_j)^3 / (1-0.8120(\theta/\theta_j) + 0.2336(\theta/\theta_j)^2 + 0.0845(\theta/\theta_j)^3) \qquad (4)$$

The results obtained with this function correlated well with simulations performed using Monte Carlo methods and experimental data obtained by Ramsden measuring the phase velocities of guided modes in optical waveguides upon which proteins were allowed to adsorb from solution.[8] The simulations yielded a saturation limit or jamming limit (θ_j) at the 54.7% which indicates the formation of a layer highly disordered. This is due to the fact that proteins can adsorb at any free position on the surface. As a consequence, adsorption on most of the remaining free positions may

be hindered after exceeding a certain coverage due to steric repulsions between solution and adsorbed proteins. This phenomenology seems more realistic than the Langmuir model which restricts the adsorption to discrete binding sites.

Expresing the surface coverage in terms of the mass density won by the system upon the adsorption (r), equation 3 turns into:

$$dr/dt = k_{ON}C_b(1-r/r_M) \quad (5)$$

where k_{ON} is the rate constant for the adsorption process in cm·min^{-1}, C_b is the bulk concentration in ng·cm^{-3}, and ρ_M the change in surface mass density in ng·cm^{-2} when the surface is completely filled and the time (t) is given in min.

Belfort et al have recently introduced a more simple form for the probability function, $\Phi(r)=(1+A@r)$,[9] in an study regarding the adsorption of proteins onto metallic surfaces. In this expression A is a constant referred to as the steric factor, i.e. a measure of the steric hindrance felt by proteins in their way to the surface. Thereby, one of the simplest forms of the so-called Random Sequential Adsorption (RSA) model can be reached by replacing $(1-\rho/p_M)$ by $(1+A\cdot\rho)$ in equation (5):

$$d\rho/dt = k_{ON}C_b(1+A\cdot\rho) \quad (6)$$

Provided that the units discussed above for the rest of parameters are kept, A is given in cm^2@ng^{-1}. Integration of this kinetic law leads to:

$$\rho=(1/A)\ (exp[2.3Ak_{ON}C_bt]-1) \quad (7)$$

Although enough evidence has been reported supporting the fact that proteins can follow the RSA mechanism under certain experimental conditions,[8,10,11] Rabe et al recently remarked that it may be insufficient in certain cases as additional effects such as conformational and orientational changes, multilayer formation, positive cooperativity, and even gravitational effects can contribute to the mechanism as demonstrated in this manuscript. This is the main reason for which further modifications have been included in this model to fit the kinetic data presented in the manuscript (experimental section).

S4. Additional data

S4.1 Washing experiments.

Buffer rinsing was performed for the films formed from most of the concentrations studied at different points of the process. The results showed negligible desorption of

the protein at any point of the process for all the concentrations investigated. Figure S7 shows the results obtained for the film formed from a relatively concentrated 13.5 $\mu g \cdot mL^{-1}$ β-LG solution. Negligible desorption can be observed at low, middle, and high times upon protein injection. Moreover, it is also demonstrated that the multiple and successive injection of protein has identical results.

S4.2 AFM images

The AFM pictures taken in tapping mode over 5 x 5 μm regions for the chitosan-modified substrates upon β-LG adsorption from solutions at different concentrations (C_b), are presented in Figures S8. The great difficulty to take good images is well illustrated in the tracks and trails observed in most of the pictures and has been appropiately discussed in the manuscript. The size of some of the features imaged have been included in red numbers. Height profiles along specific directions of the surface, noted in the images, have been included in order to have an estimation on the size of these features.

S4.3 DD_5 vs $Df_5/5$ plots

Figure S9 presents the dissipation and frequency changes simultaneously measured upon injection of the corresponding protein solutions within the concentration range studied.

S5. Figures

Scheme S1. Sketch illustrating the strategies implemented for the preparation of chitosan-modified surfaces and the subsequent adsorption of β-LG. The arrows describe the different steps of the modification consisting on substrate immersion in the solutions indicated over the arrows (more details in the experimental section). The AUT SAM is represented by brown S heads, gray organic chains and blue $-NH_2$ endgroups. The gray and green sinusoidal ribbons correspond to ideal representations of pSS and Chitosan polyelectrolytes. The large cyan spheres in the last draw represent the β-LG protein. The charge borne by these species depends, obviously, on the solution pH. The size of some features has been highlighted for better clarity.

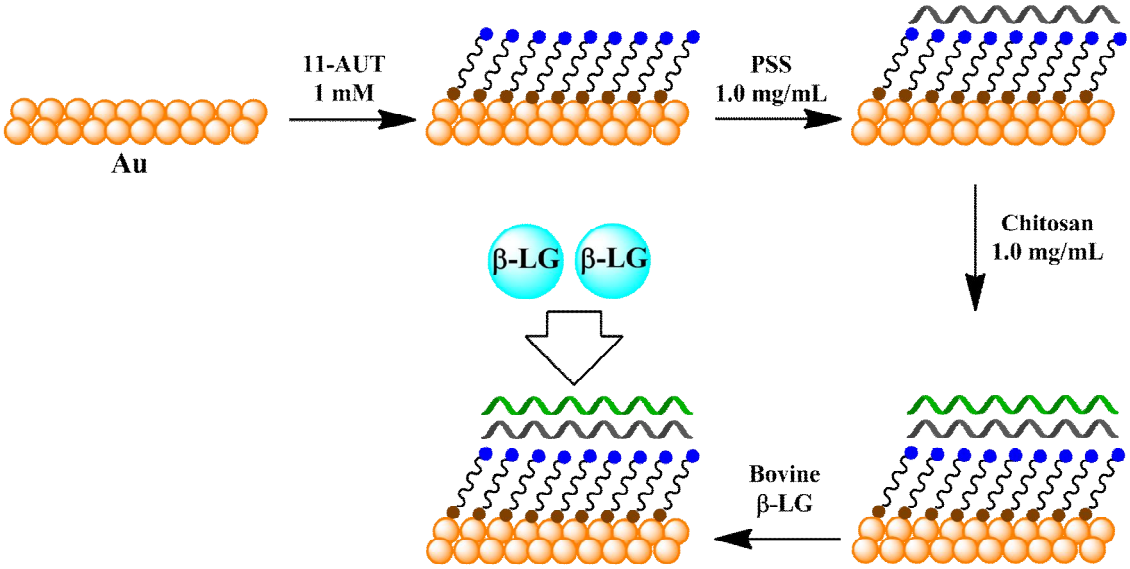

Figure S1. Time resolved shift in the surface mass uptake sensed by a 5 MHz quartz crystal plate upon the injection of 11-AUT 1 mM, PSS 1 mg.mL^{-1}, and Chitosan 1 mg.mL^{-1} in 0.05 M acetate buffered solution (pH = 5.5). The mass was calculated from the normalized $Df_5/5$ data using the Sauerbrey´s equation.

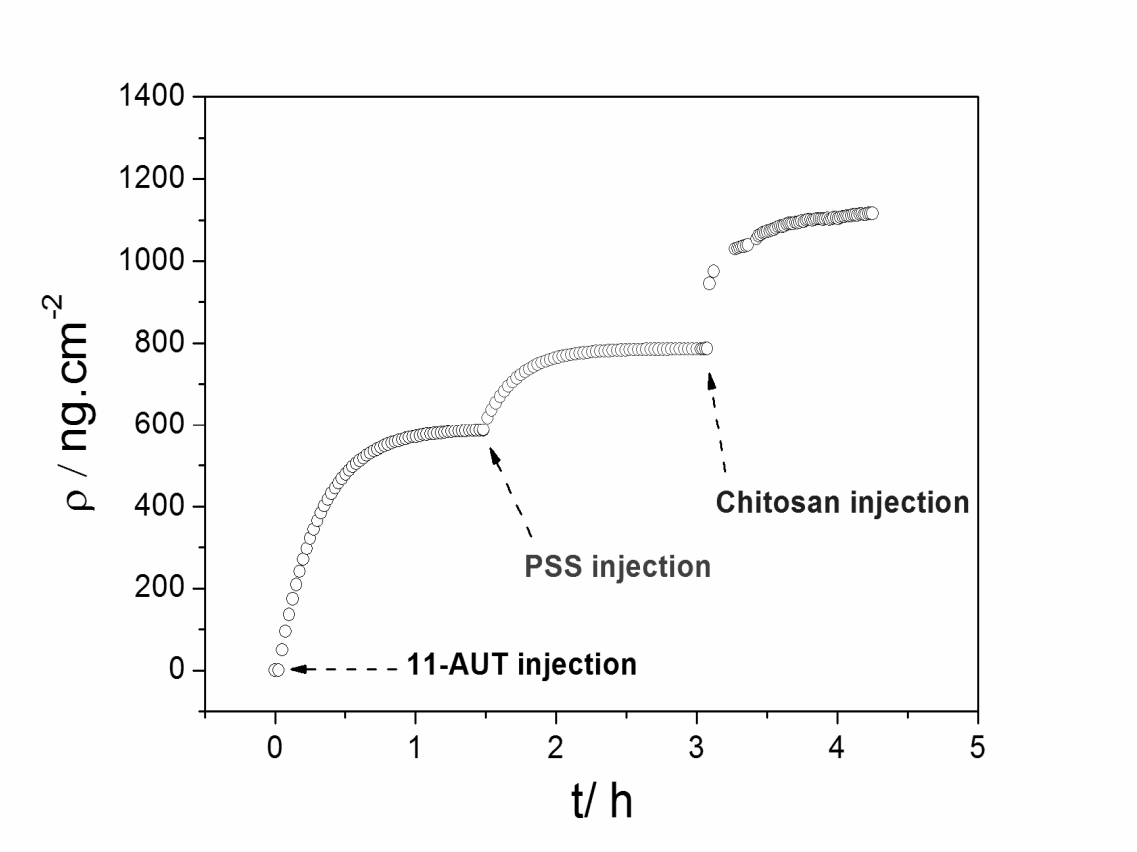

Figure S2. Dissipation factor shift (DD_n) measured at different overtones (n), 5 (black line), 7 (red), and 9 (blue), after the consecutive injection of the following solutions: 1 mM AUT in ethanol (A); 1 mg·mL^{-1} pSS in acetate buffer 0.05 M at pH=5.5 (B); and 1 mg·mL^{-1} chit95 in acetate buffer 0.05 M at pH=5.5 (C). The samples were removed from the QCM-D cell and dried under nitrogen between each of these experiments. The values obtained after equilibration in each of the solvents were subtracted to get the corresponding baselines.

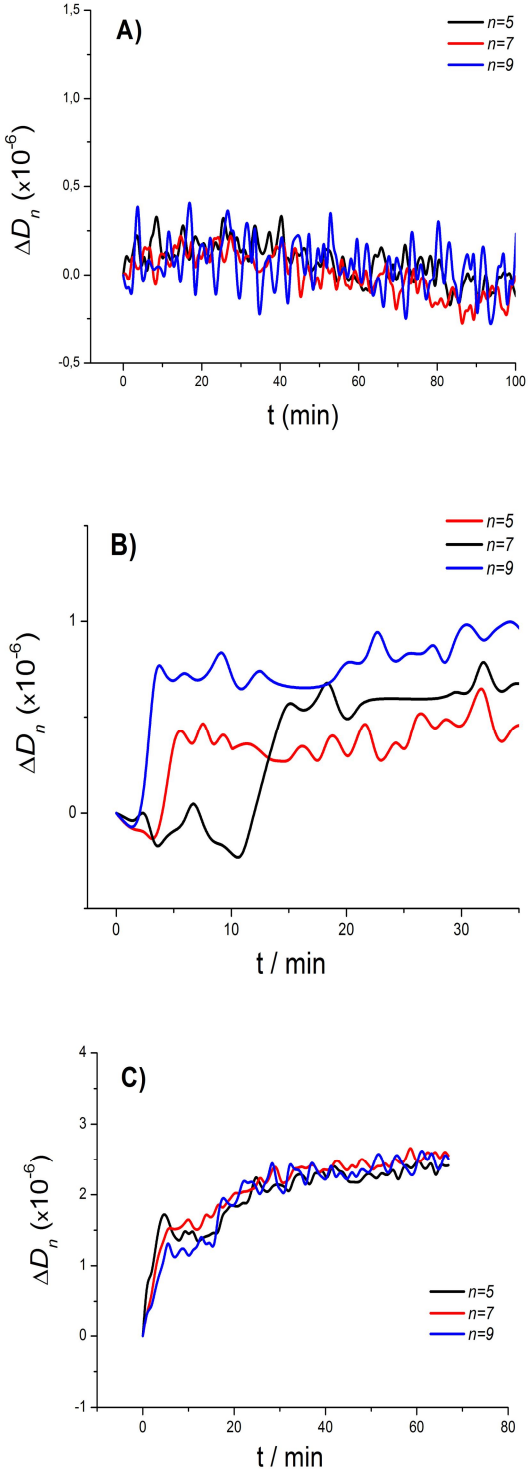

Figure S3. AFM images taken in tapping mode over 5 x 5 μm^2 regions of the quartz plates modified with Au (A), Au/AUT (B), Au/AUT/pSS (C) and Au/AUT/pSS/Chit95 (D). The regions displayed were representative of the full samples. The height profiles along the white lines drawn in the images have been also extracted in each case.

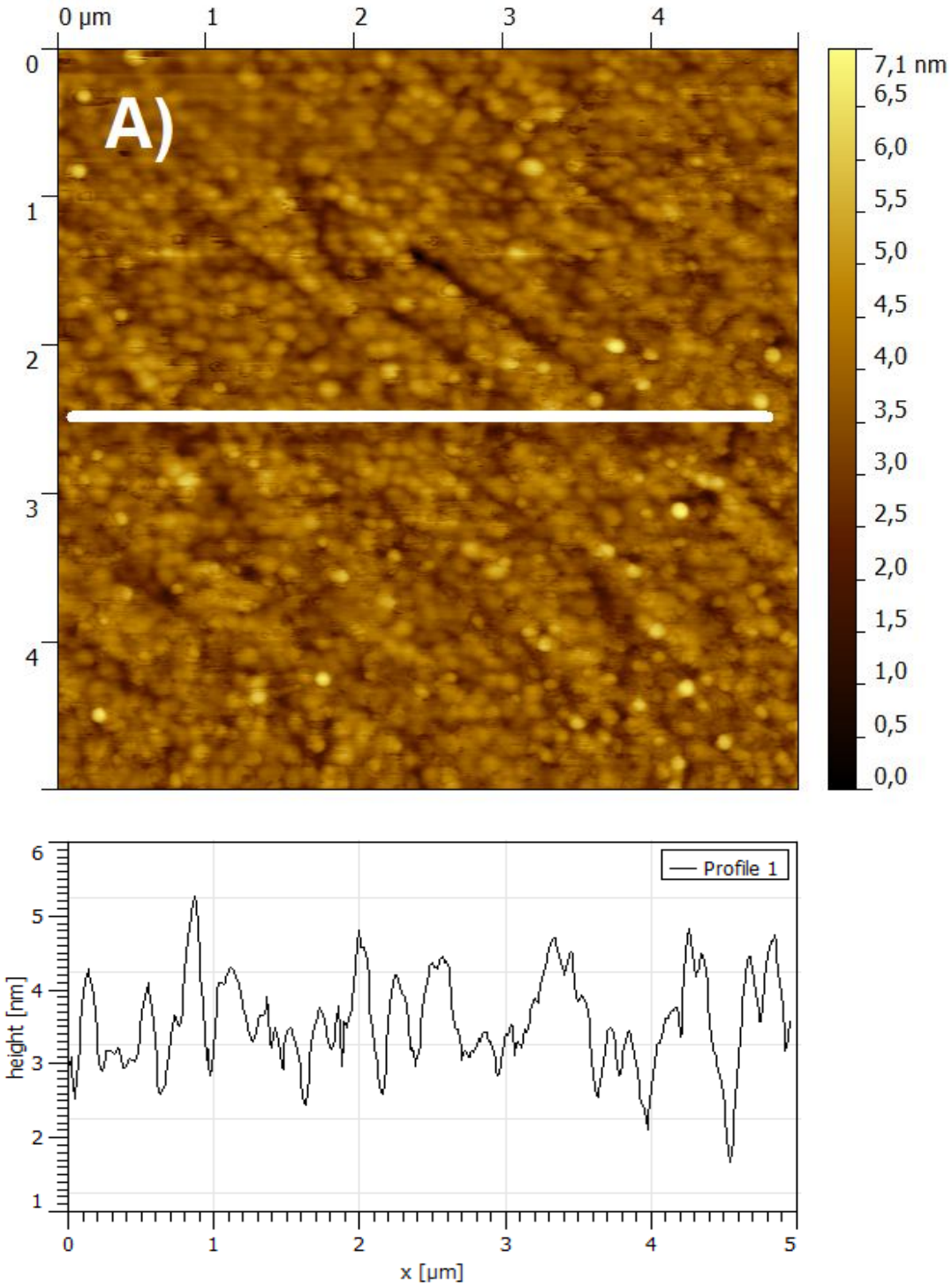

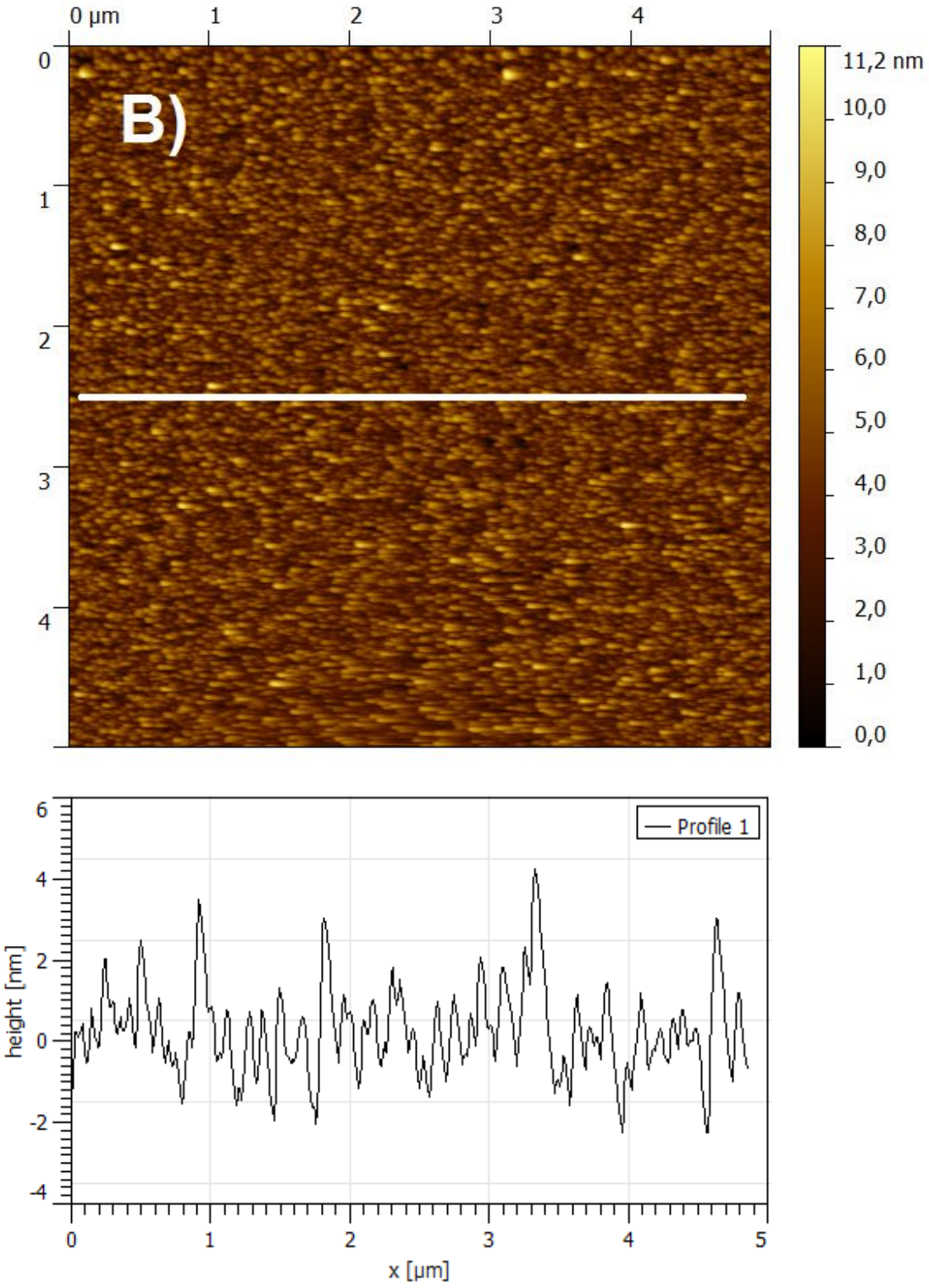

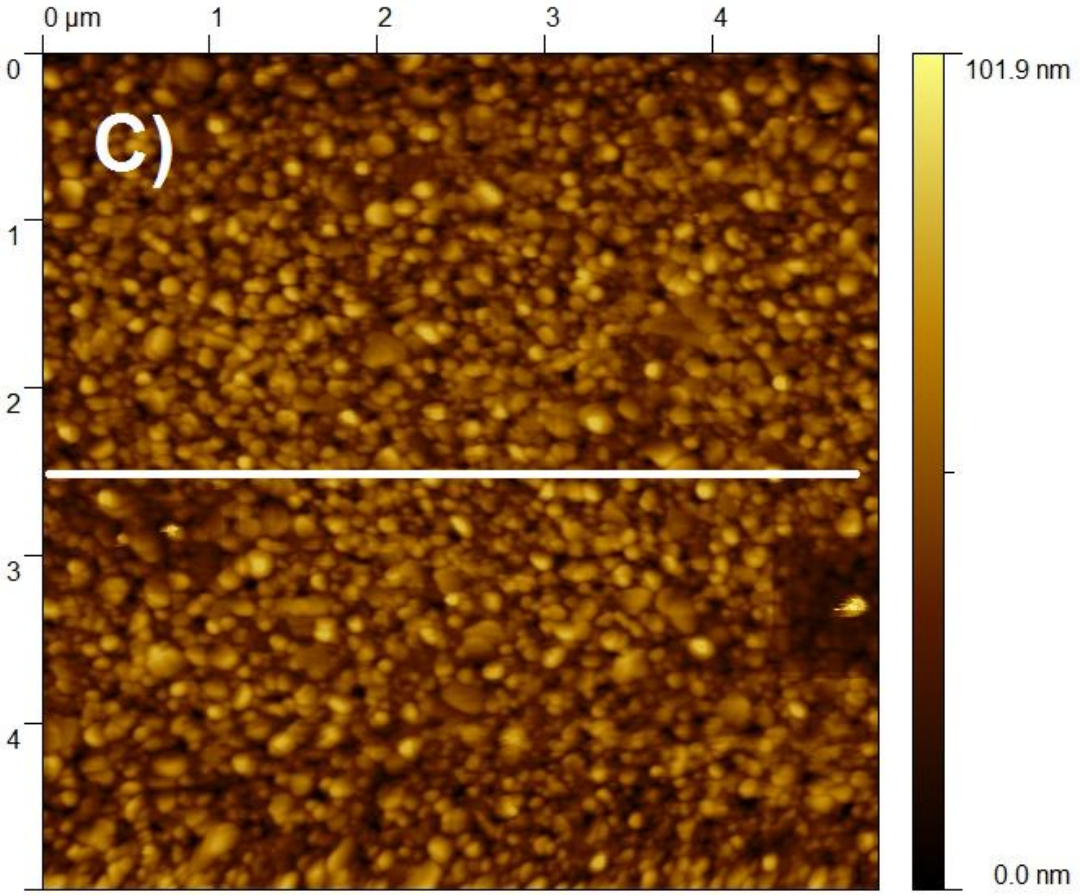

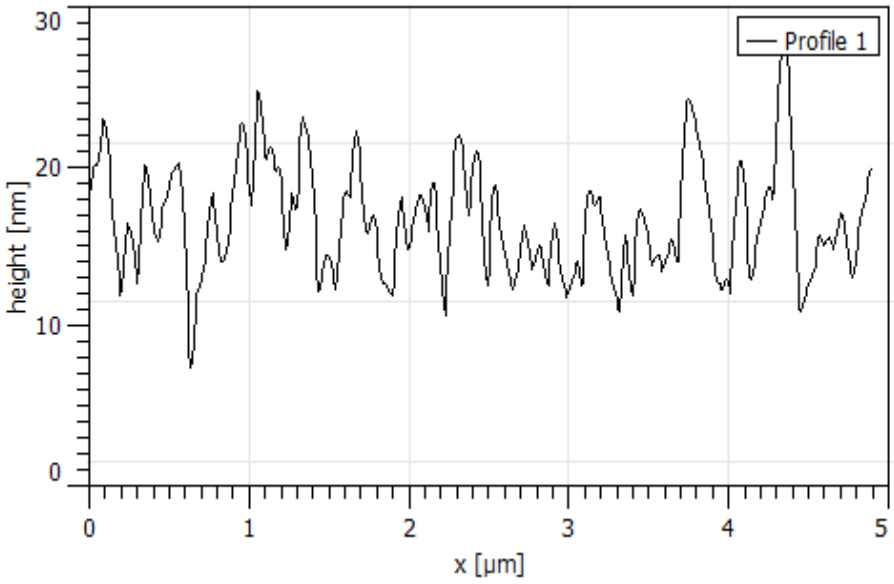

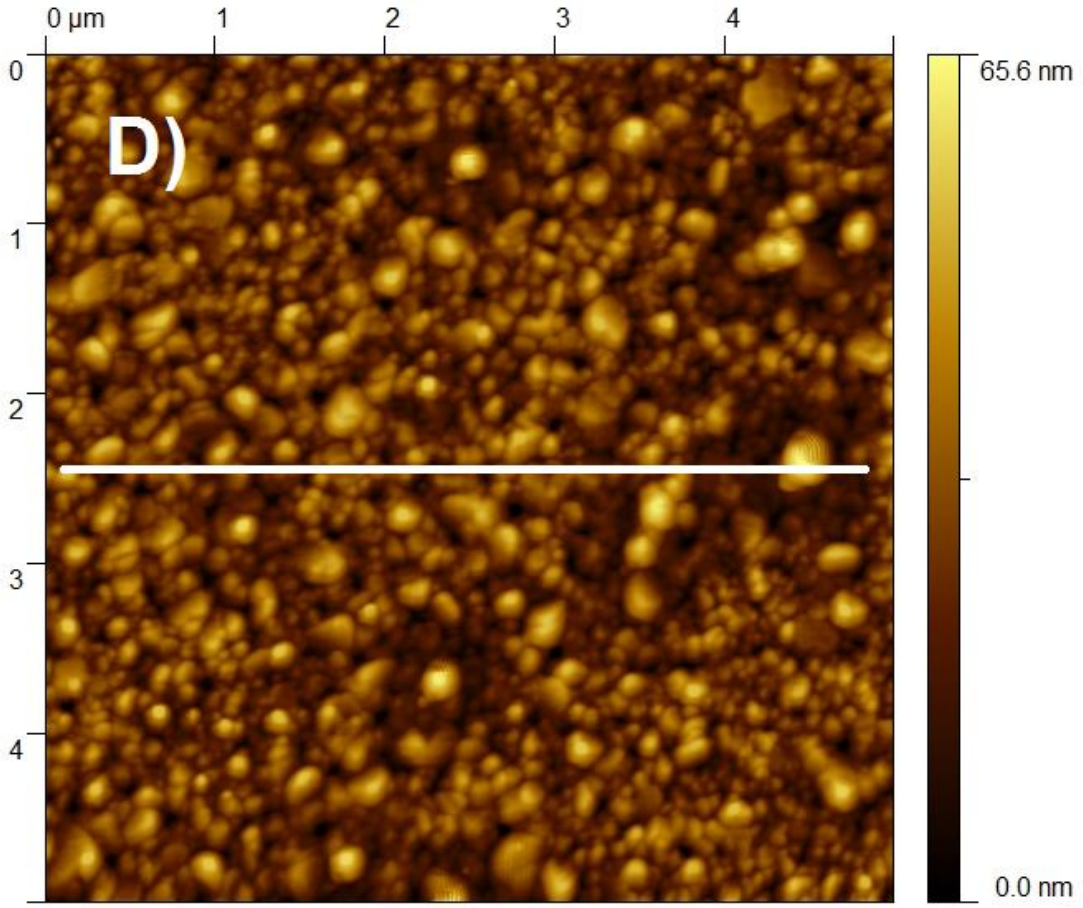

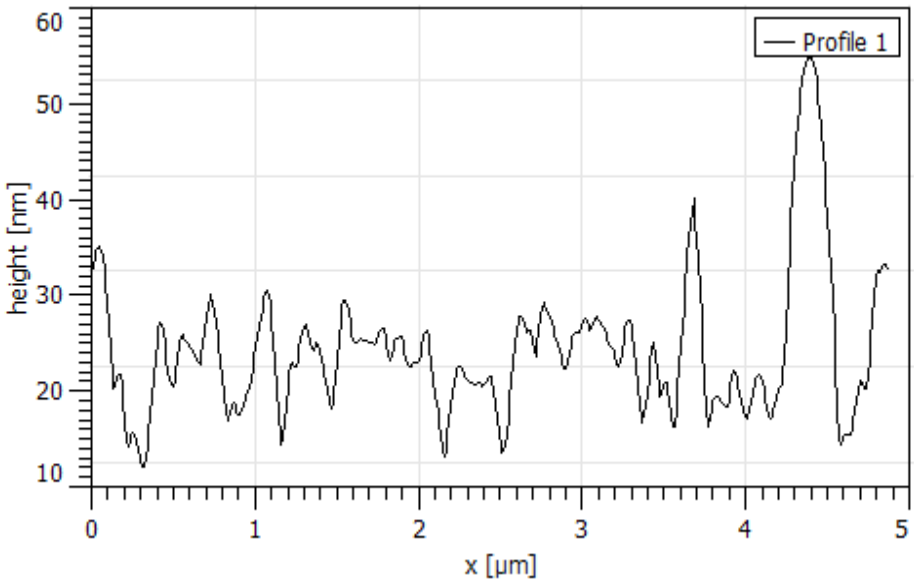

Figure S4. SEM images taken in high-vacuum (20 kV) and SE mode over different regions of the quartz plates modified with Au/AUT/pSS (A) and Au/AUT/pSS/Chit95 multilayers (B). The regions displayed were representative of the full samples. The magnification factor was 50000 x and WD 8.8 mm in both cases.

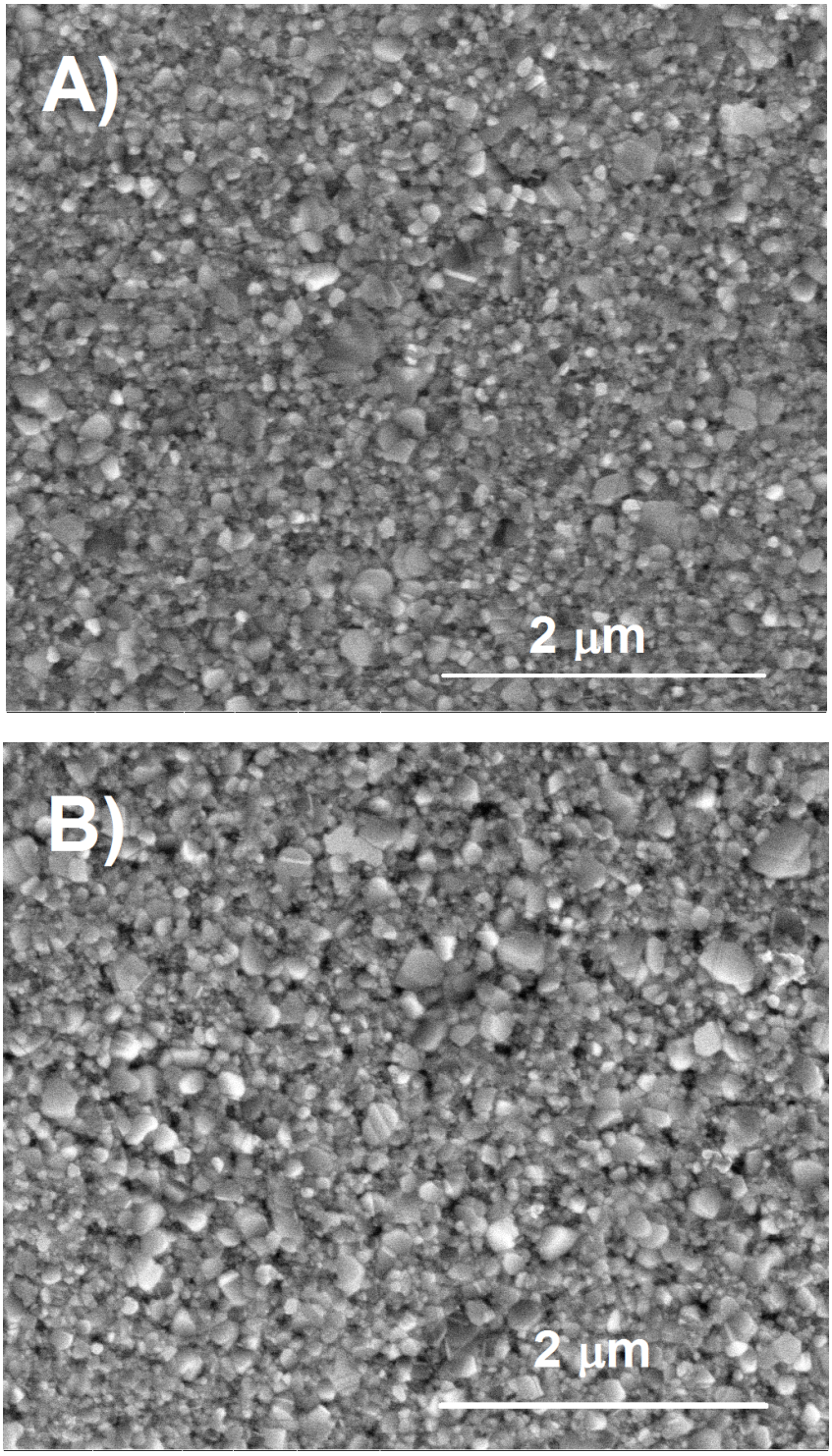

Figure S5. Changes in the contact angle measured for Au surfaces modified with AUT (B), AUT/pSS (C), AUT/pSS/Chit95 (D), and AUT/pSS/Chit95/β-LG after adsorption from 0.01 (E) or 50.0 $\mu g\,mL^{-1}$ (F) acetate buffered protein solutions (pH=5.5). The picture for sessile drop on bare Au (A) is included for comparison.

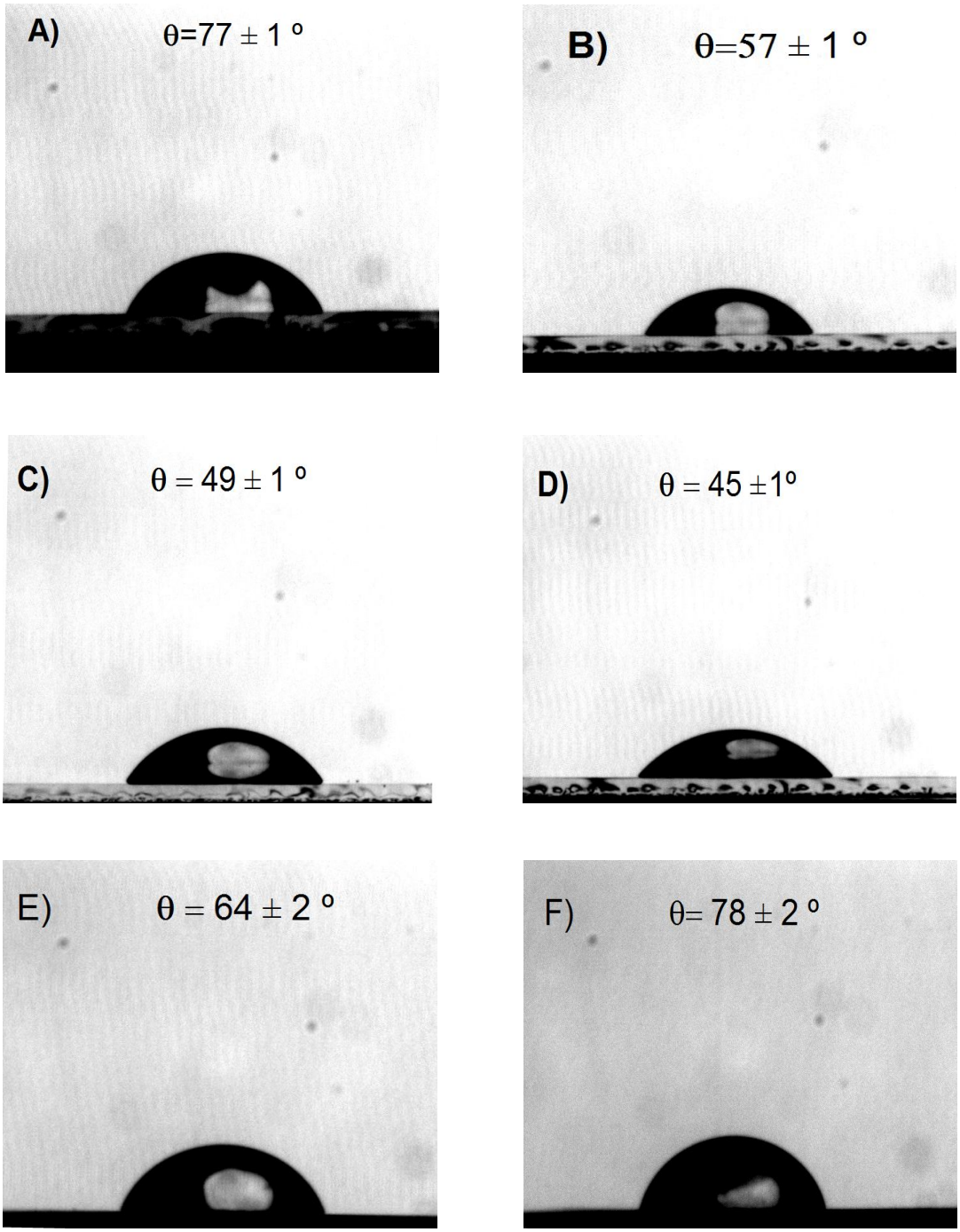

Figure S6. Evolution in the adsorption rate ($d\Gamma/dt^{-1}$) of β-LG from 0.01 (a), 0.2 (b), 0.5 (c), 2.5 (d), and 13.5 μg mL^{-1} (e) solutions in acetate buffer (*pH=5.5, I=50 mM*) versus their corresponding mass uptake (Γ). The rate decreases in all cases with a different slope after exceeding a certain critical mass uptake (Γ_{crit}) as indicated by the black straight lines.

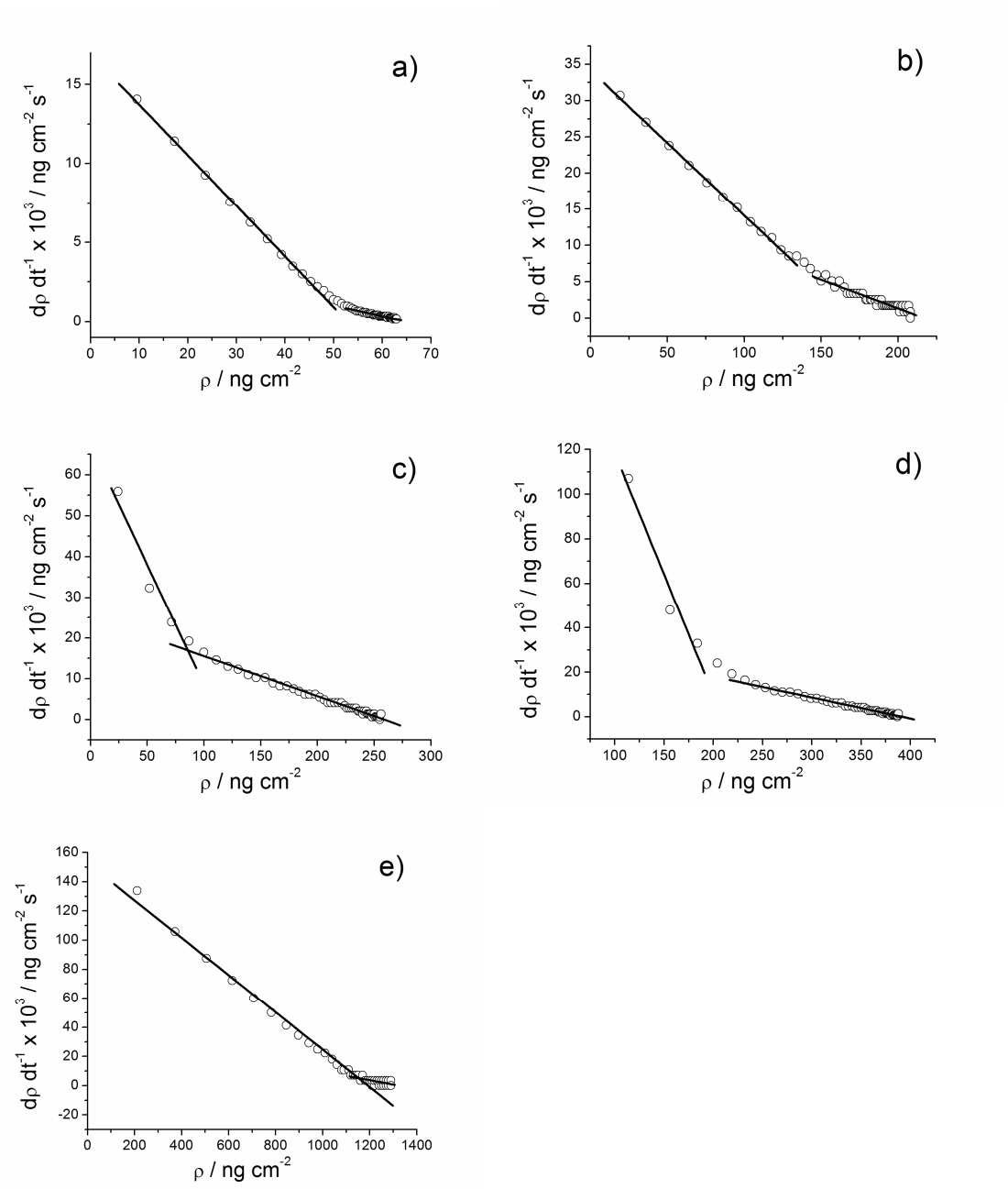

Figure S7. Frequency shift registered in the fifth overtone ($\Delta f_5/5$) during the adsorption of β-LG (black line) from a 13.5 $\mu g\,mL^{-1}$ solution in acetate buffer 0.05 M (pH=5.5). The experiment was repeated under identical conditions but injecting buffer solution at different points of the adsorption process as indicated by the colored arrows: after 500 s (red line), 12000 s (blue line), and 80000 s (green line). The inset shows a detailed view of the latter experiment. Multiple buffer injections (as indicated by the black arrows) did not show to have a significant effect in the magnitude of $\Delta f_5/5$.

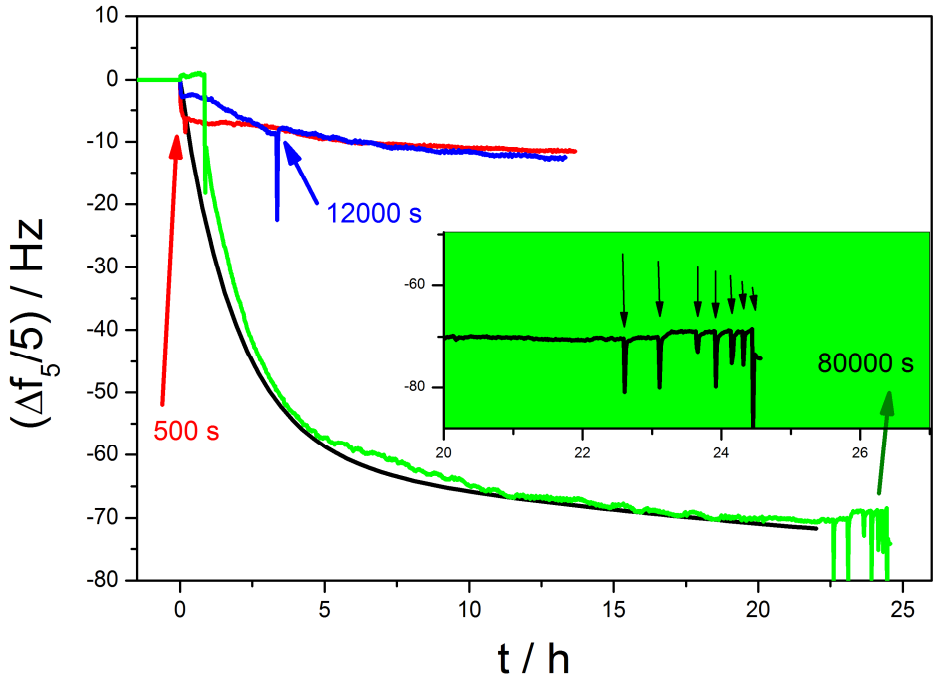

Figure S8. AFM images taken in tapping mode for the Au-covered quartz plates modified with a AUT/pSS/chit95 multilayer upon the adsorption of β-LG from 0.05 M acetate buffer solutions (pH=5.5) with the following concentrations: 0.2 (a), 1.0 (b), 4.5 (c), 9.0 (d), and 50.0 $\mu g \cdot mL^{-1}$ (e). The size was 5 x 5 μm^2 in all cases.

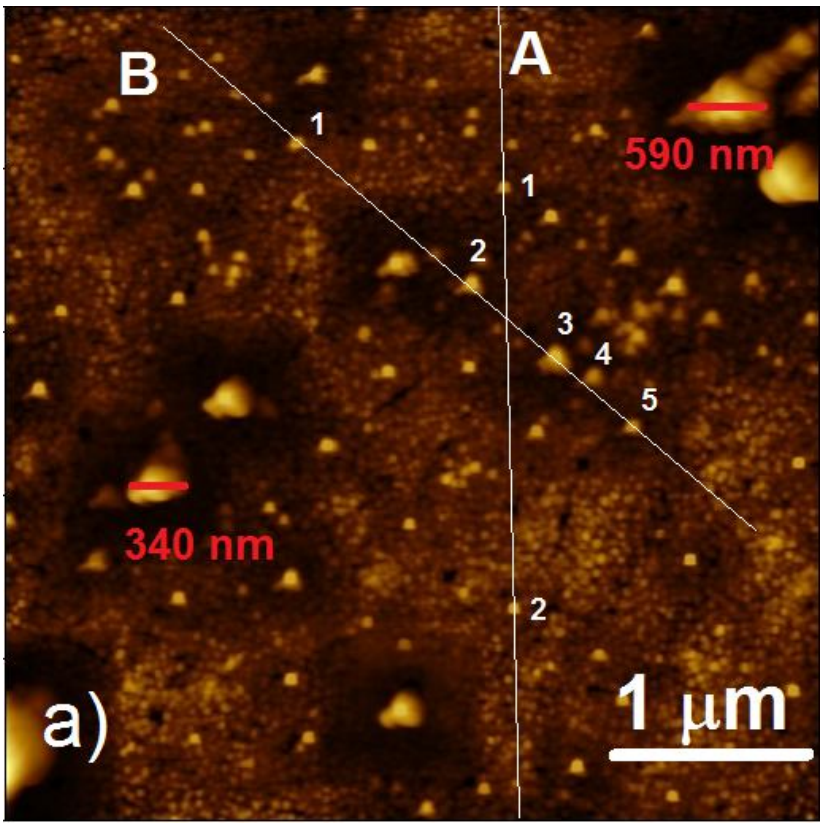

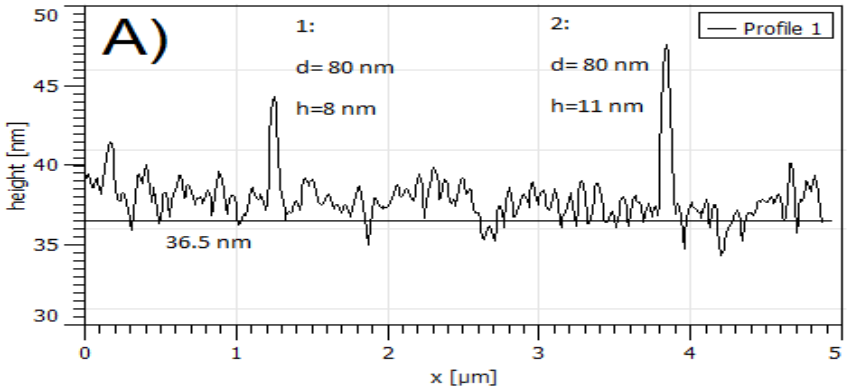

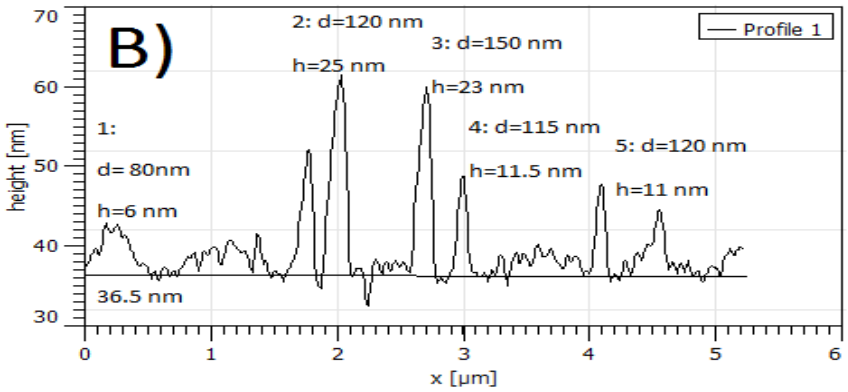

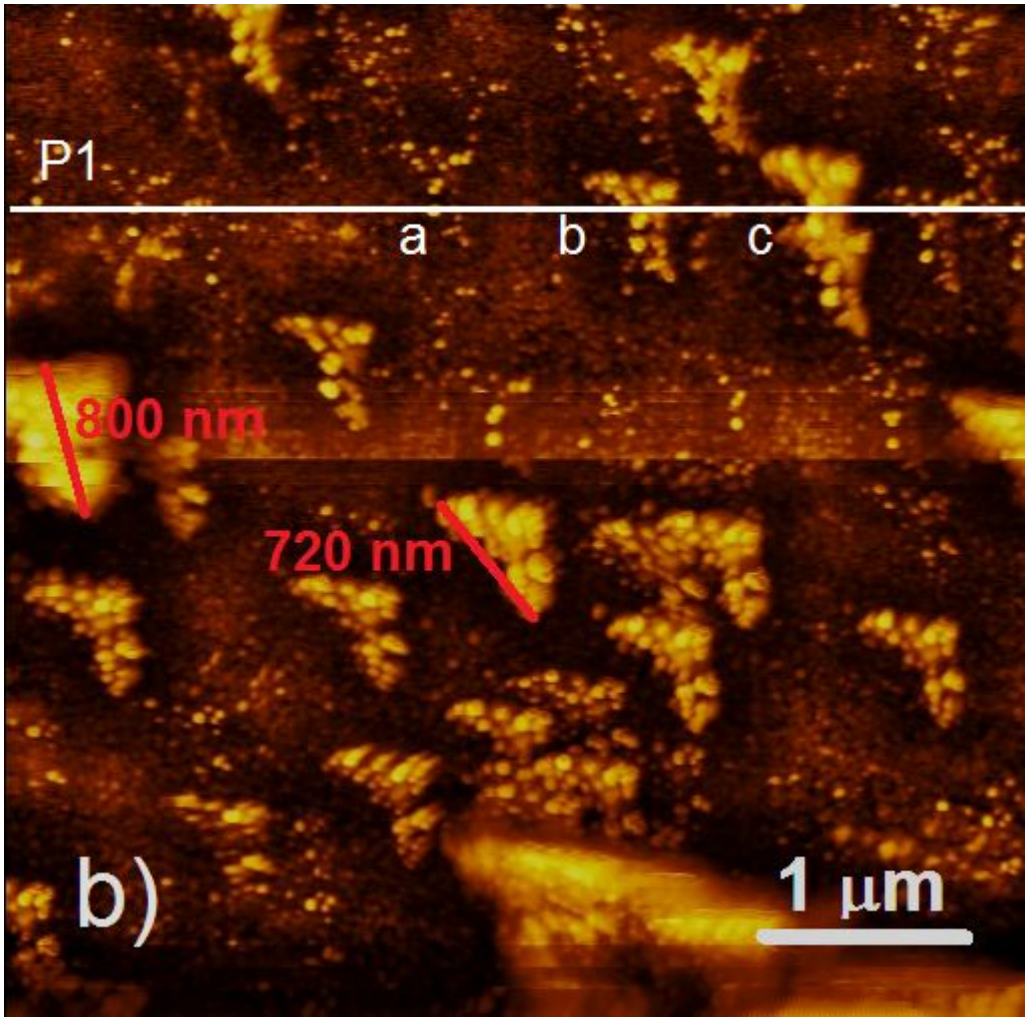

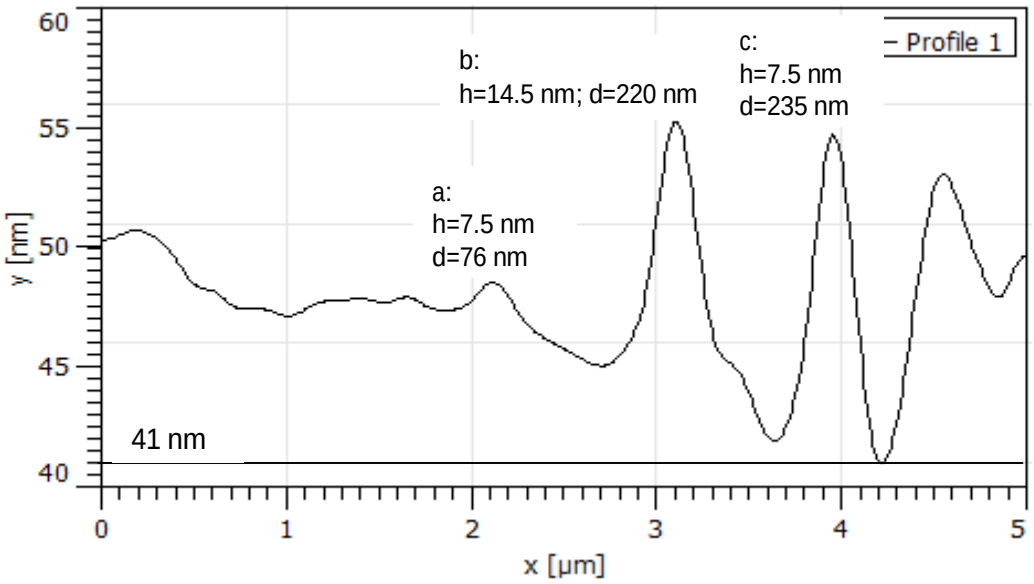

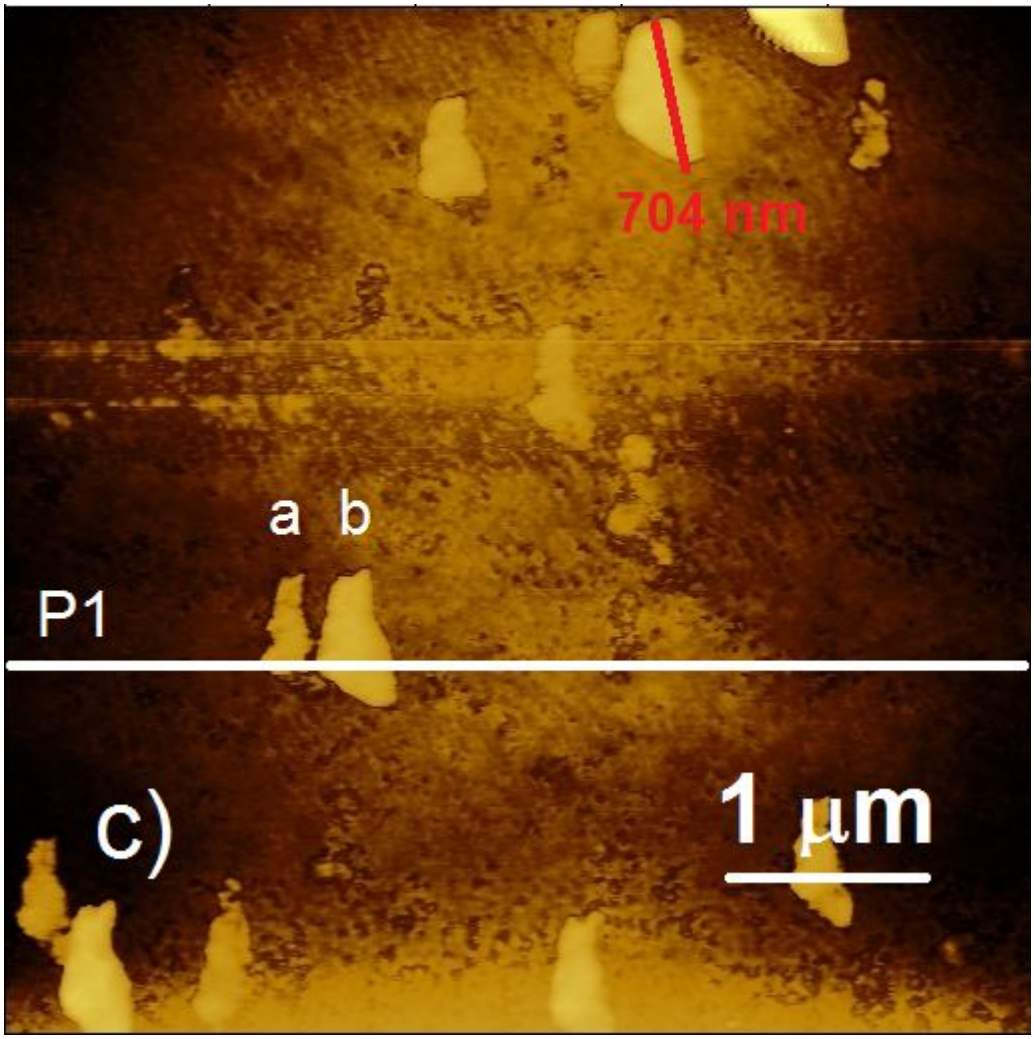

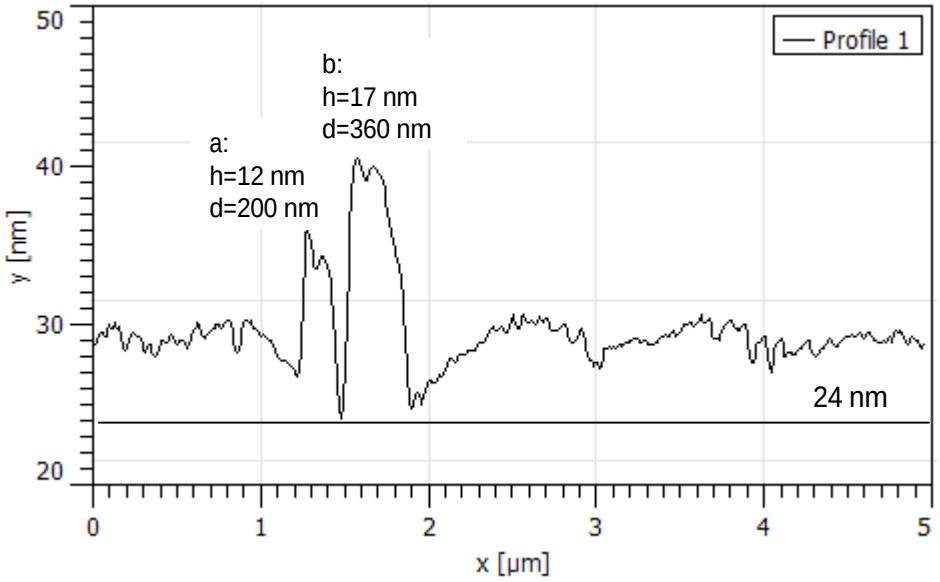

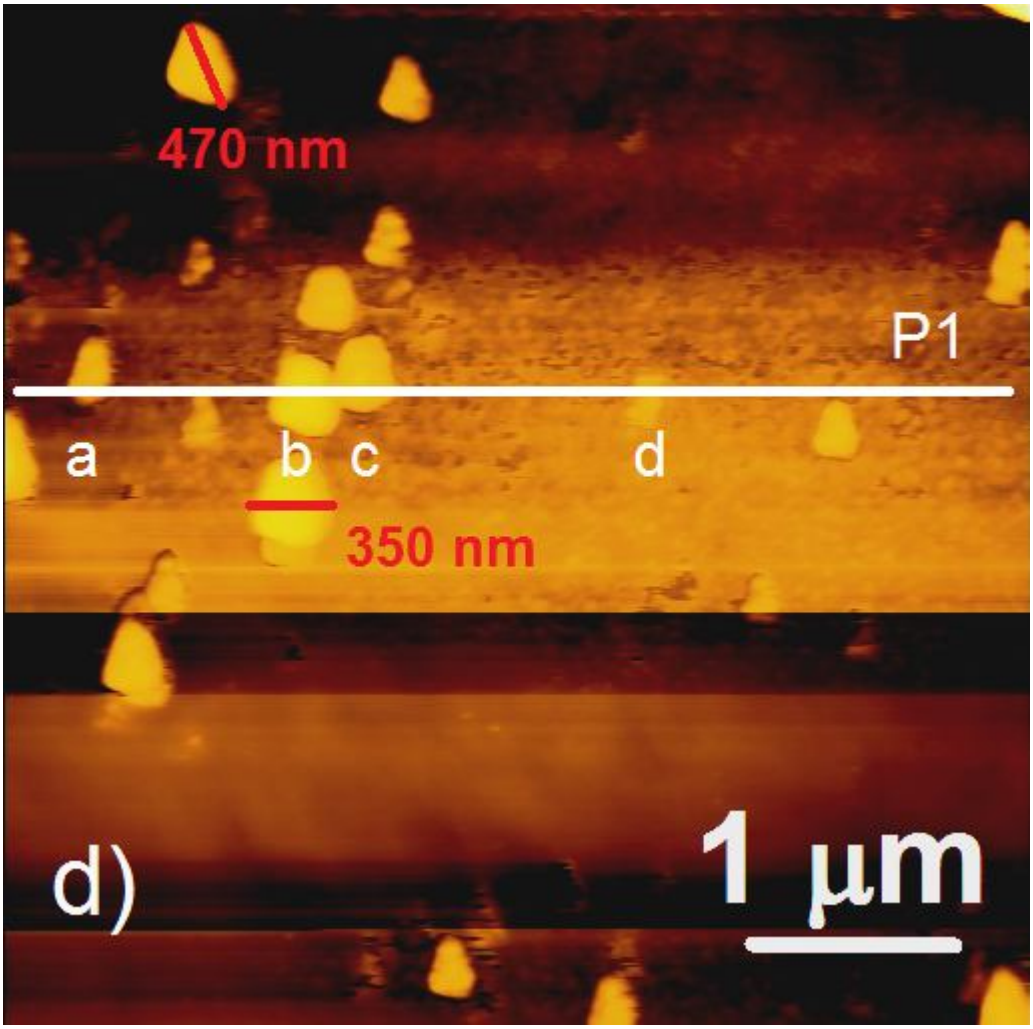

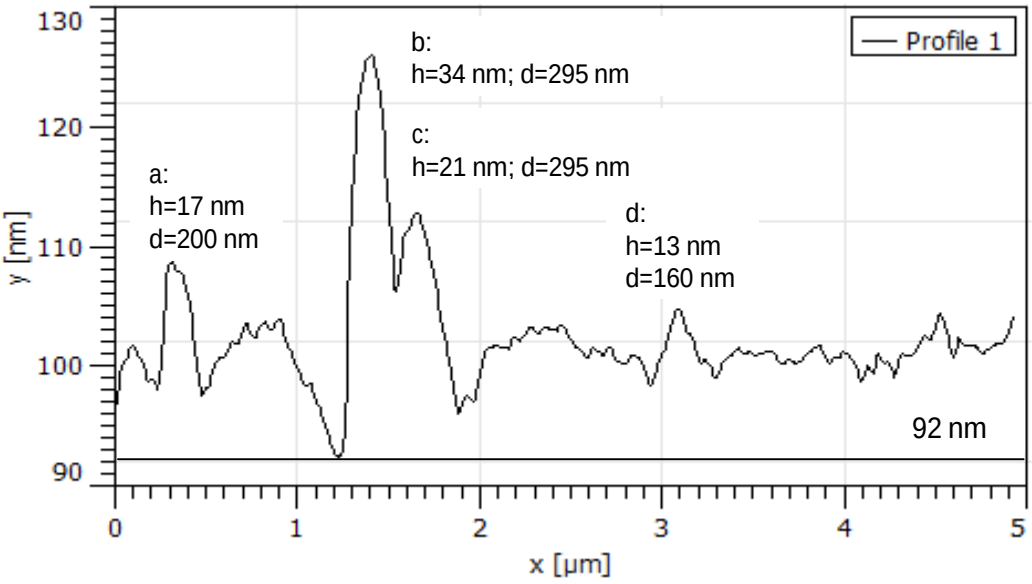

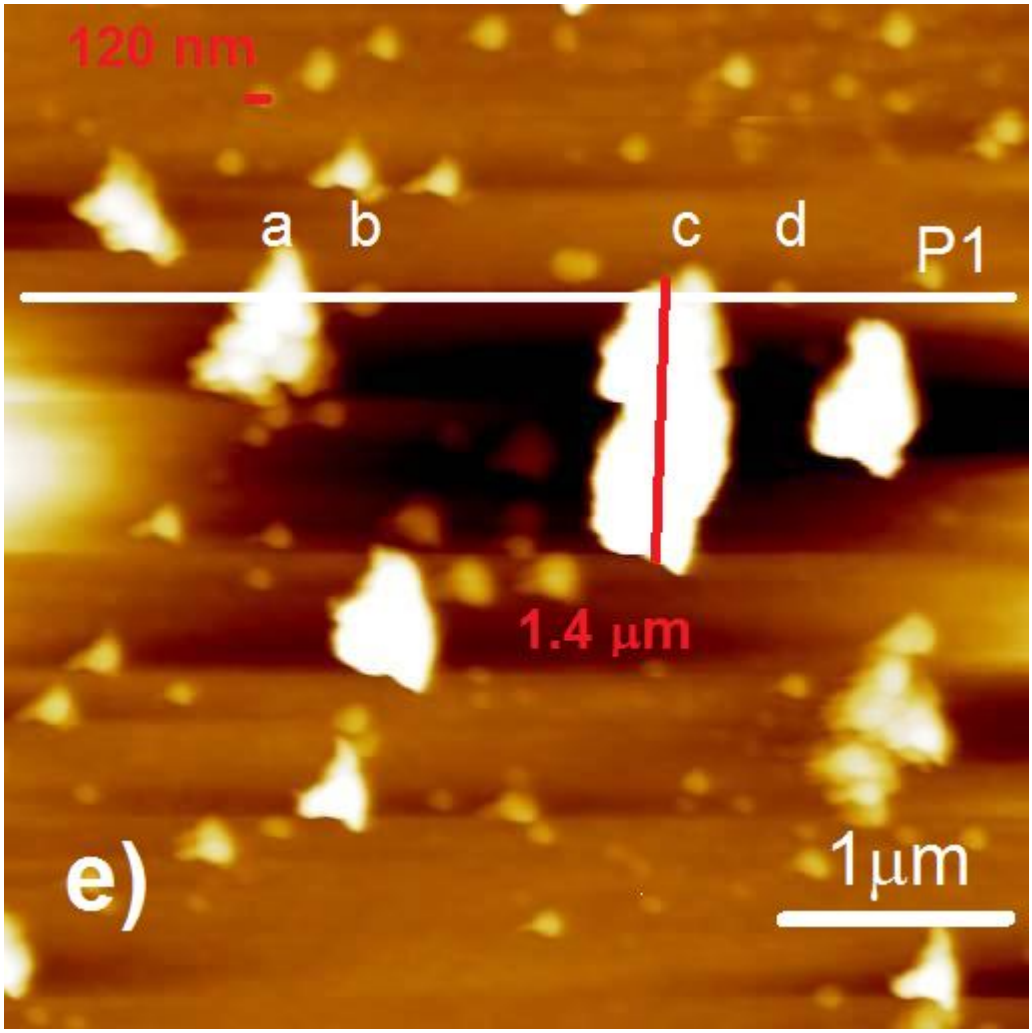

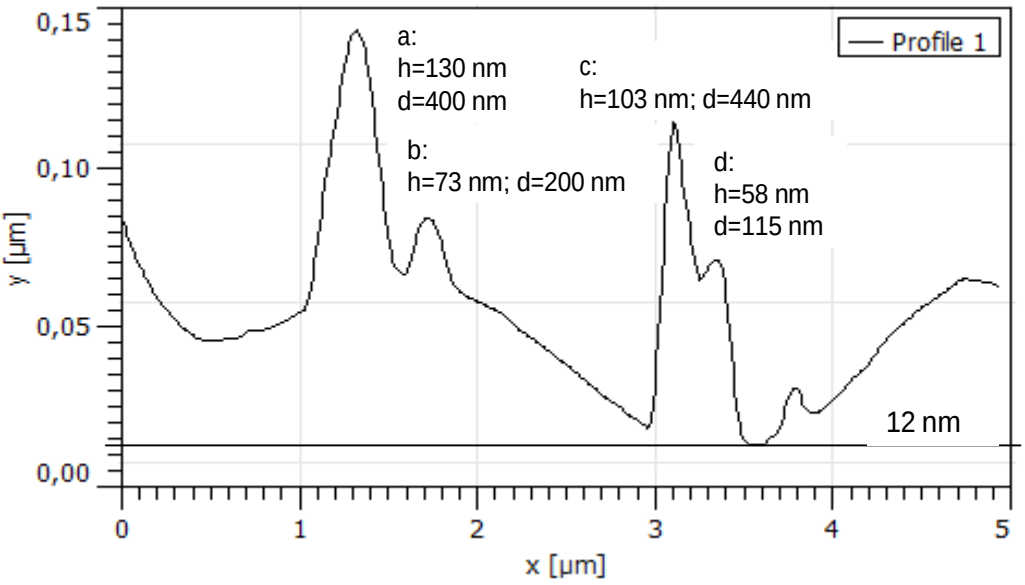

Figure S9. *DD vs DF* plots built for the fifth overtone from the QCM-D data sense by the different quartz crystals after the injection of 0.05 M acetate buffered (pH=5.5) β-LG solutions with the following concentrations: (A) 0.01 (black data), 0.2 (red), 1.0 (green), 2.5 (blue), 4.5 $\mu g \cdot mL^{-1}$ (orange), and (B) 9.0 (black), 13.5 (red), 25.0 (green), and 50.0 $\mu g \cdot mL^{-1}$ (blue).

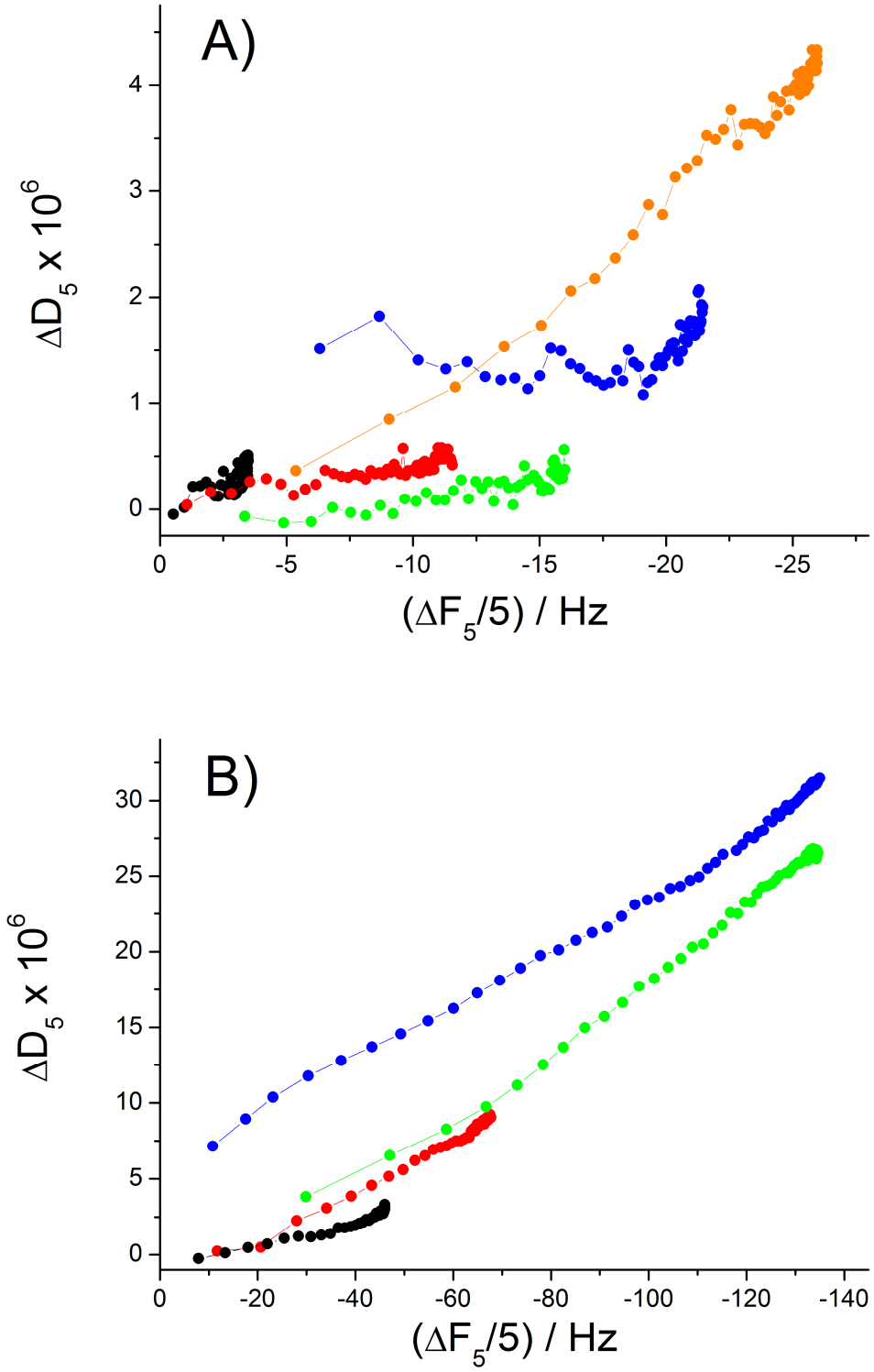

Table S1. Some statistical parameters: the root-mean-square surface roughness (R_{ms}), the average height (H_{AV}), and the range of apparent particle diameters (d_{PART}); calculated from the AFM images presented in Figure S3 by means of the software Gwyddion 2.24.

Sample	R_{ms} / nm	H_{AV} / nm	d_{PART} / μm
Au	2.08	3.82	<0.08-0.09
Au/AUT	1.22	4.86	<0.06
Au/AUT/pSS	7.30	24.3	<0.15
Au/AUT/pSS/Chit95	6.29	18.3	<0.20-0.30

S6. References

[1] G. Sauerbry, Zeitschrift für Physik, 1959, **155**, 206.

[2] J. M. Campiña, H. K. S. Souza, J. Borges, A. Martins, M. P. Gonçalves, F. Silva, Electrochim. Acta, 55 (2010) 8779.

[3] B. S. Murray, L. Cros, Colloid Surface B, 10 (1998) 227; B. S. Murray and C. Deshaires, J. Colloid Interface Sci. 227 (2000) 32.

[4] A. Baba, F. Kaneko, R. C. Advíncula, Colloids Surface A, 173 (2000) 39.

[5] N. F. Ferreyra, L. Coché-Guerénte, P. Labbé, E. Calvo, V. M. Solís, Langmuir, 19 (2003) 3864.

[6] A. Rényi, Publ. Math. Inst. Hung. Acad. Sci. 3 (1958) 109.

[7] P. Schaaf, J. Talbot, J. Chem. Phys., 91 (1989) 4401.

[8] J. J. Ramsden, Phys. Rev. Lett., 71 (1993) 295.

[9] G. Anand, S. Sharma, A. K. Dutta, S. K. Kumar, G. Belfort, Langmuir, 26 (2010) 10803.

[10] M. Rabe, D. Verdes, J. Zimmermann, S. Seeger, J. Phys. Chem. B, 112 (2008) 13971.

[11] J. Talbot, G. Tarjus, P. R. Van Tassel, P. Viot, Colloids Surf. A, 165 (2000) 287.